Periodic elastic nanodomains in ultrathin tetragonal-like $BiFeO_3$ films

Zhenlin Luo,[1,*,†] Zuhuang Chen,[2,†] Yuanjun Yang,[1] Heng-Jui Liu,[3] Chuanwei Huang,[2] Haoliang Huang,[1] Haibo Wang,[1] Meng-Meng Yang,[1] Chuansheng Hu,[1] Guoqiang Pan,[4] Wen Wen,[5] Xiaolong Li,[5] Qing He,[5] Thirumany Sritharan,[2] Ying-Hao Chu,[3] Lang Chen,[2,6,‡] and Chen Gao[1,§]

[1]*National Synchrotron Radiation Laboratory and CAS Key Laboratory of Materials for Energy Conversion, Department of Materials Science and Engineering, University of Science and Technology of China, Hefei 230026, China*

[2]*School of Materials Science and Engineering, Nanyang Technological University, Singapore 639798, Singapore*

[3]*Department of Materials Science and Engineering, National Chiao Tung University, Hsinchu 30010, Taiwan*

[4]*National Synchrotron Radiation Laboratory, University of Science and Technology of China, Hefei 230026, China*

[5]*Shanghai Synchrotron Radiation Facility, Shanghai Institute of Applied Physics, Chinese Academy of Sciences, Shanghai 201204, China*

[6]*Department of Physics, South University of Science and Technology of China, Shenzhen 518055, China*

(Received 31 December 2012; revised manuscript received 20 May 2013; published 26 August 2013)

We present a synchrotron grazing incidence x-ray diffraction analysis of the domain structure and polar symmetry of highly strained $BiFeO_3$ (BFO) thin films grown on $LaAlO_3$ substrate. We reveal the existence of periodic elastic nanodomains in the pure tetragonal-like BFO ultrathin films down to a thickness of 6 nm. A unique shear strain-accommodation mechanism is disclosed. We further demonstrate that the periodicity of the nanodomains increases with film thickness but deviates from the classical square root law in the ultrathin thickness regime (6–30 nm). Temperature-dependent experiments further reveal the disappearance of periodic modulation above ∼90 °C due to a M_C-M_A structural phase transition.

DOI: 10.1103/PhysRevB.88.064103 PACS number(s): 77.80.bn, 61.05.cp

I. INTRODUCTION

With the miniaturization trend of functional devices, nanoscale epitaxial ferroic (ferroelectric, ferromagnetic, ferroelastic, etc.) thin films have gained great attention in recent years due to their fundamental physics and practical applications in, for example, sensors and information storage.[1] Domains form in ferroic films to minimize the free energy of depolarizing (or demagnetizing) fields and elastic film-substrate interaction (epitaxial strain).[2] For instance, epitaxial strain due to lattice mismatch between film and an underlying substrate creates a driving force for the formation of regular elastic (non-180°) domains in ferroic films grown on single-crystal substrates.[3–7] Such elastic domain was predicted theoretically by Roitburd in 1976,[3] and was experimentally observed in tetragonal $PbTiO_3$,[8] $Pb(Zr_xTi_{1-x})O_3$,[9] $BaTiO_3$,[10] rhombohedral $BiFeO_3$ (BFO),[11] orthorhombic $NaNbO_3$,[12] and Aurivillius layered $SrBi_2Ta_2O_9$ (Ref. 13) epitaxial ferroelectric films. Domain structure plays a crucial role in determining the physical properties of ferroic thin films.[2] Furthermore, recent studies have revealed that domain walls themselves present unique functionalities[14] such as enhanced conductivity[15] and magnetism.[16] Therefore, understanding and controlling the ferroic domain structure, especially in ultrathin films, is of importance to realize the practical applications. However, regarding ferroelectrics, most previous experimental studies focused on relatively thick films with dense domain structure,[7] while the domain structure and domain size evolution with film thickness in ultrathin films have been less thoroughly investigated. This is mainly because probing the domain structure in ultrathin films is challenging. Scanning probe techniques do not readily provide sufficient resolution to detect domain structure in ultrathin ferroelectric films because of the weak piezoelectric response and fine domain feature of the ultrathin films. Transmission electron microscopy has been used instead, but it is destructive and might change the electric and mechanical boundary conditions and thus may not provide the original structural information, especially for the highly strained films.[17] Recently, synchrotron grazing incidence x-ray diffraction (GIXRD) techniques have been used successfully to probe nanoscale 180° ferroelectric stripe domains in $PbTiO_3$ ultrathin films as the periodic nanodomains produce satellite peaks in x-ray scattering.[18–20] The distribution and orientation of these satellites from nanodomains in reciprocal space can provide rich information on the domain structure and polar symmetry in ferroelectric ultrathin films.[18–21]

Among ferroic materials, BFO is of particular interest because of its lead-free nature, large ferroelectric polarization, robust piezoelectricity, room temperature multiferroic properties, and relatively small band gap.[22] The crystal and domain structures of rhombohedral BFO films have been extensively studied in the past decade.[22,23] Recently, a "super tetragonal" BFO phase with a giant axial ratio and a huge spontaneous polarization was predicted by theoretical studies,[24] and experimentally confirmed in highly strained BFO films grown on $LaAlO_3$ (LAO),[25–27] $LaSrAlO_4$,[28] $NdAlO_3$,[29] and $YAlO_3$ substrates.[26] The crystal structure of this super tetragonal BFO at room temperature was determined to be tetragonal (T) -like M_C-type monoclinic with Pm or Pc symmetry.[27,30,31] Besides the giant polarization,[32] a near-room-temperature multiferroic phase transition from the M_C phase to a high-temperature T-like monoclinic M_A phase was reported for T-like BFO films more recently, implying potential applications of this unusual T-like phase.[33–36] However, despite recent intensive studies on T-like BFO films,[25–39] the detailed domain structure and its temperature and thickness dependence, and the strain-accommodation mechanism in these highly strained films, especially in ultrathin pure T-like films, have not yet been fully understood. This hinders full understanding of the structure-property relationship and the accuracy of inferences on the magnetoelectric coupling in the recently discovered super tetragonal phase.

In this paper, we report observations of unique periodic elastic stripe nanodomains and their thickness and temperature dependence using synchrotron x-ray diffraction in a series of sub-30-nm-thick T-like BFO ultrathin films grown on (001)-oriented LAO substrates. We also demonstrate that the stripe domain period increases with the film thickness but deviates from the classical square root law, and the M_C phase transforms to a pure T-like M_A phase at ~90 °C simultaneously with the disappearance of the periodic domains.

II. EXPERIMENTAL METHODS

Epitaxial BFO thin films with thicknesses ranging from 2 to 30 nm were grown on (001)-oriented $LaAlO_3$ (LAO) single-crystal substrates using pulsed laser deposition at 700 °C under an oxygen pressure of 100 mTorr.[28] The crystallographic structure of the films was studied using high-resolution synchrotron x-ray diffraction from two sources: the BL14B1 beamline of the Shanghai Synchrotron Radiation Facility (SSRF, λ=1.2398 Å) for conventional reciprocal space mappings (RSMs) and the U7B beamline of the Hefei National Synchrotron Radiation Laboratory (NSRL, λ = 1.537 Å) for GIXRD studies.[40] The RSMs were plotted in reciprocal lattice units (r.l.u.) of the LAO substrate (1 r.l.u. = $2\pi/3.789$ Å^{-1}) and the diffraction intensity was indicated by different colors (low to high: blue, green, yellow, red, gray). Film thickness was determined by analyzing synchrotron x-ray reflectivity data.[40]

III. RESULTS AND DISCUSSION

Previous studies have revealed that the pure T-like phase only occurs in BFO films of thickness less than 30 nm grown on LAO, while a larger thickness leads to multiphase coexistence due to strain relaxation.[26,37] Here, all films display atomically flat terraces with single-unit-cell steps in the atomic force microscopy topography.[37,40] Figure 1 shows typical RSMs in pseudocubic coordinates around (002) and (0$\bar{1}$3) reflections for a 10-nm-thick film. Only peaks from the substrate and the BFO film with an out-of-plane lattice parameter of 4.64 Å were

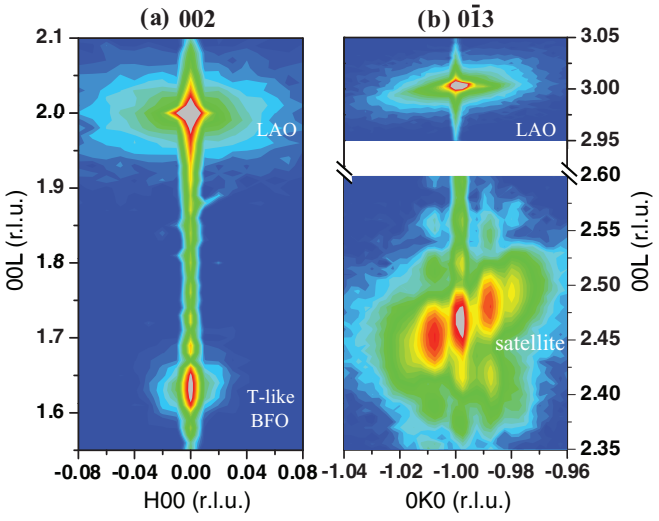

FIG. 1. (Color online) RSMs around (002) and (0$\bar{1}$3) reflections for a 10-nm-thick BFO film on LAO.

detected, indicating that the film is pure tetragonal-like. The presence of thickness fringes along the L direction indicates that the film is very smooth, which is consistent with the topography data.[37,40] As shown in Fig. 1(b), satellite peaks with identical spacing are observed around the 0$\bar{1}$3 Bragg peak of the film, implying the existence of periodic domains in the film. Further, both the central and the satellite peaks show thickness fringes, indicating that the periodic domains extend through the entire film. The lack of satellite peaks around pure out-of-plane reciprocal lattice points ($H = K = 0$, $L \neq 0$), such as (002) shown in Fig. 1(a), suggests that the relative positional shift of atoms in adjacent domains lies horizontally without any out-of-plane component.

In order to get more information about the in-plane domain structures, the GIXRD technique was adopted to map out the in-plane reciprocal space. Figure 2 shows typical RSMs around various in-plane reciprocal lattice points for the 10-nm film, measured in grazing incidence geometry. These RSMs are proportionally enlarged to show details. Obviously, satellites are observed around all $HK0$ reciprocal lattice points. The satellites around 010/020 Bragg peaks are aligned along both in-plane diagonal directions ([110] and [$\bar{1}$10]), while the satellites around 220/$\bar{2}$20 peaks lie only along one direction ([$\bar{1}$10] or [110]). Analysis of the diffraction data reveals that the reflections originate from two sources: domain variants of T-like BFO and periodic alignment of these domains.[41] For instance, comparing the ($\bar{1}$10) RSM with the ($\bar{2}$20) one, it could be deduced that (1) the outer major diffraction spots, fallen on lines converging to the origin, are reflections from the same family of crystallographic planes but with different orders, and (2) the inner satellite spots with identical spacing stand for a superlatticelike structure of periodic nanodomains. The oval profile of domain reflections indicates that stripe domains aligned along the [$\bar{1}$10] direction and the splitting can be attributed to the twinned structure of the LAO substrate. The satellites' spacing value yields an in-plane periodicity of ~30 nm. After detailed analysis of all RSMs, the origins of all reflection spots are identified and marked in Fig. 2. Since the diffraction intensity profile shown in these RSMs comes from the convolution integral of the diffractions from crystal domains as well as the domain's periodic modulation, peak overlap is inevitable, which is especially obvious in the (010) and (020) RSMs.

Figure 2 shows that the modulations due to periodic nanodomains are along the ⟨110⟩ directions, which are perpendicular to the domain wall orientations revealed by piezoelectric force microscopy (PFM).[27] This can be interpreted by a model of periodic M_C domains with antiphase in-plane rotations, as shown in Fig. 3. Figures 3(a)–3(c) show the orientation relationship between the in-plane lattices of the film and the substrate. For quantitative analysis, in-plane lattice parameters of $a = 3.833(3)$ Å, $b = 3.747(3)$ Å extracted from a 24-nm-thick BFO film are used, since the lattice parameters of the pure T-like films stay almost constant.[28,40] The in-plane rotations of adjacent M_C domains are determined to be $\pm 0.661°$ ($\pm 0.005°$) from the relative shift of BFO (020) reflection from the LAO [010] axis.[40] Calculation shows that the film lattice is coherent with that of the LAO substrate along one diagonal direction [110]/[$\bar{1}$10] after rotation, where the lattice constants match by ~99.9% and the angle difference is only

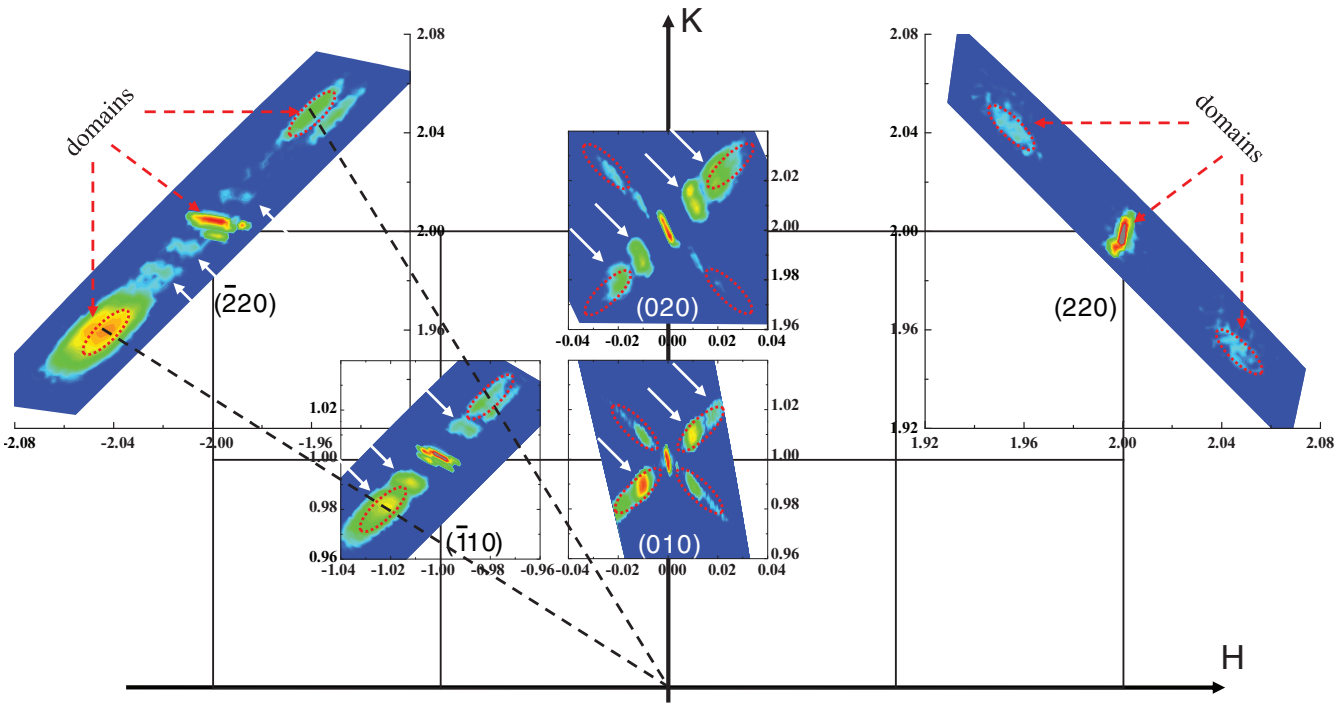

FIG. 2. (Color online) In-plane RSMs of the 10-nm-thick BFO film. These RSMs are proportionally enlarged. Red arrows and red circles indicate the reflections of domain variants while white arrows indicate those of periodic modulation.

0.01°. The domain pattern observed in the reciprocal space, as illustrated in Fig. 3(d), is in good agreement with the fourfold in-plane alignment symmetry of the M_C domain variants and two choices of in-plane rotation proposed here. The domain structure is composed of a rotated domain (marked as domain A in Fig. 3) and another adjacent antiphase equal-angle rotated domain (marked as domain B in Fig. 3). The observed in-plane periodic modulation along [110]/[$\bar{1}$10] could be attributed to one-dimensional periodic alignment of such M_C domain twins with domain walls lying along [$\bar{1}$10]/[110]. Two cases ("head to tail" and "head to head") of possible periodic domain structures with domain walls along the ⟨110⟩ directions in real space and the corresponding simulated satellite around ($\bar{1}$10) in reciprocal space are illustrated in Fig. 3(e) for the M_C phase, where each case assumes the presence of four domain structures due to the fourfold symmetry of a (001)-oriented pseudocubic substrate. The observed satellites in ($\bar{1}$10) RSM for our T-like BFO films are consistent with the "head to tail" case where domain walls are uncharged. The satellites due to periodic domains are only evident around reciprocal lattice points with in-plane component (H $\neq$ 0 or K $\neq$ 0). This suggests that the periodic nanodomains are pure elastic ones and have the same out-of-plane polarization component, which is consistent with the out-of-plane PFM image that shows a uniform contrast.[27,37,40] The periodic elastic nanodomain pattern observed here is different from the ferroelectric 180° stripe domain structure found in $PbTiO_3$ ultrathin films in order to reduce the depolarization energy.[18–20] In addition, it is important to note that the satellite spots are not caused by the twinned substrate, because the twin size of the LAO substrate is much larger, on the order of tens of micrometers, than the modulation period exhibited in the RSMs. This claim is further confirmed by supplementary experiments in which we found no existence of lattice modulation from bare LAO substrate after similar heat treatment.[40]

Based on the above discussion, it is clear that the GIXRD RSMs obtained here present a sum effect of the M_C domain variants and the periodic modulation of nanodomain twins, which discloses a unique strain-accommodation mechanism of the highly strained pure T-like BFO film on LAO, i.e., stripe M_C BFO domains with small antiphase in-plane rotations lying periodically in the film along one ⟨110⟩ direction with uncharged domain walls. The shear strain due to the unit-cell rotation could be further diminished by a hierarchical structure constructed from the alternation of the two groups of periodic M_C domains, as shown in Figs. 3(a) and 3(b). A similar hierarchical structure of four twins has been predicted by Roytburd in 1993 for tetragonal ferroelectric thin films.[4,5]

To investigate the thickness-dependent domain structure of T-like BFO films, GIXRD was performed on films with various thicknesses. Overall the profiles of the in-plane RSMs were similar to that of the 10-nm BFO film. Typical RSMs of the 24- and 30-nm films are shown in Fig. 4. It could be noted that these BFO films are pure T-like except for the 30-nm film, where the appearance of a weak reflection spot at the bottom of Fig. 4(d) signifies a minority rhombohedral-like phase. It also should be noted that, with the increasing film thickness, the relative intensities of domain reflections become larger while those of the periodic modulation reflections become weaker with a smaller interval. This can be attributed to increasing domain size leading to bigger modulation periodicity in thicker films. Moreover, as clearly shown in the ($\bar{1}$10) RSMs, positional shift of the domain reflections is not obvious ($\ll$1%), indicating an unchanging lattice constant of the M_C phase. The stripe

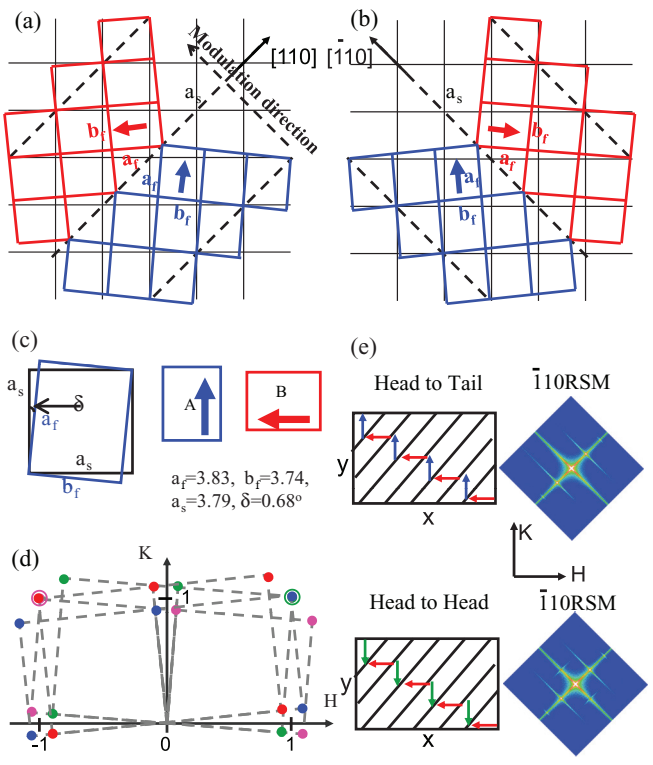

FIG. 3. (Color online) (a)–(c) Schematic diagram of lattice matching between M_C domain twins (A and B) and the LAO substrate. Arrows represent the in-plane polarization vectors of domains. (d) Sketch of all M_C domain variants in reciprocal space ($L = 0$ plane). (e) Illustration of two cases of possible periodic domain structures of ferroelectric M_C phase in real space and the corresponding simulated satellites in ($\bar{1}10$) RSMs, on (001)-oriented pseudocubic substrate.

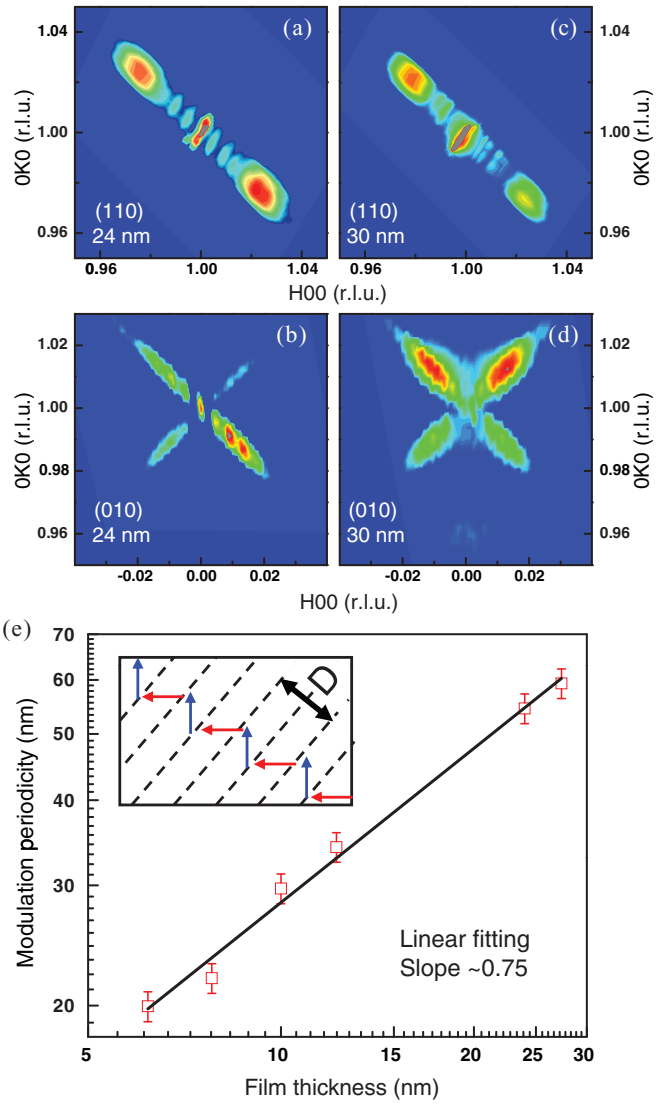

FIG. 4. (Color online) In-plane RSMs around (010) and (110) reflections for the 24-nm (a), (b) and 30-nm (c), (d) BFO films. (e) Periodicity of in-plane stripe domain as a function of film thickness for the T-like BFO films at room temperature. The domain pattern is illustrated in inset.

domain period D in the pure T-like BFO films is plotted in Fig. 4(e) in a log-log scale as a function of film thickness d. Notably, for the T-like films with thickness below 30 nm, the domain period D scales with the film thickness d, obeying a power law $D \propto d^{\gamma}$, with a scaling exponent $\gamma \approx 0.75 \pm 0.05$. In epitaxial ferroic films, the stripe domain periodicity generally experiences a nonmonotonous thickness-dependent evolution,[4,14,42–44] including three distinct regions:[44] (i) a classical square root law ($\gamma = 0.5$) for thick films where the film thickness d is much larger than the domain periodicity D, (ii) a deviation from the square root law for intermediate film thickness, and (iii) an increase exponentially in ultrathin films when decreasing film thickness. For thick ferroic films, where the domain size is much smaller than the film thickness (i.e., dense domain structure), the domain size scales with the square root of film thickness, which has been clarified in ferromagnetics by Kittel,[45] ferroelectrics by Mitsui and Furuichi,[46] and ferroelastics by Roitburd.[3–5] For intermediate films (region II), the domain size becomes comparable to the film thickness, which leads to a significant increase of the electrostatic interaction from the films surfaces. Consequently, the domain size scaling behavior starts to diverge from the classical law. This is in reasonable agreement with our observed deviation of square root scaling behavior in the pure T-like BFO films below 30 nm, where the size of the M_C domain is comparable with the film thickness. Furthermore, no satellites due to periodic domains were detected in a 2-nm BFO ultrathin film, indicating that the film is likely to be monodomain (region III).

Thermally driven evolution of the T-like phase and its domain pattern was investigated by temperature-dependent GIXRD. The results obtained in a 12-nm-thick BFO film are shown in Fig. 5. Figures 5(a)–5(f) present the ($\bar{1}10$) and (010) RSMs at 100 °C, 80 °C, and 25 °C, respectively. The outer domain reflection peaks disappear at 100 °C simultaneously with the superlattice satellites, while the central one becomes stronger in intensity, indicating a structural phase transition occurring between 80 °C and 100 °C. Detailed rocking curves of ($\bar{1}10$) reflection ($2\theta = 33.4°$) were measured at different temperatures and shown in Fig. 5(g). Below 85 °C, the dependence of satellite spacing on temperature is relatively weak. At ~85 °C, there are abrupt changes in both intensity and position of the satellite peaks and outer reflection peaks of the M_C

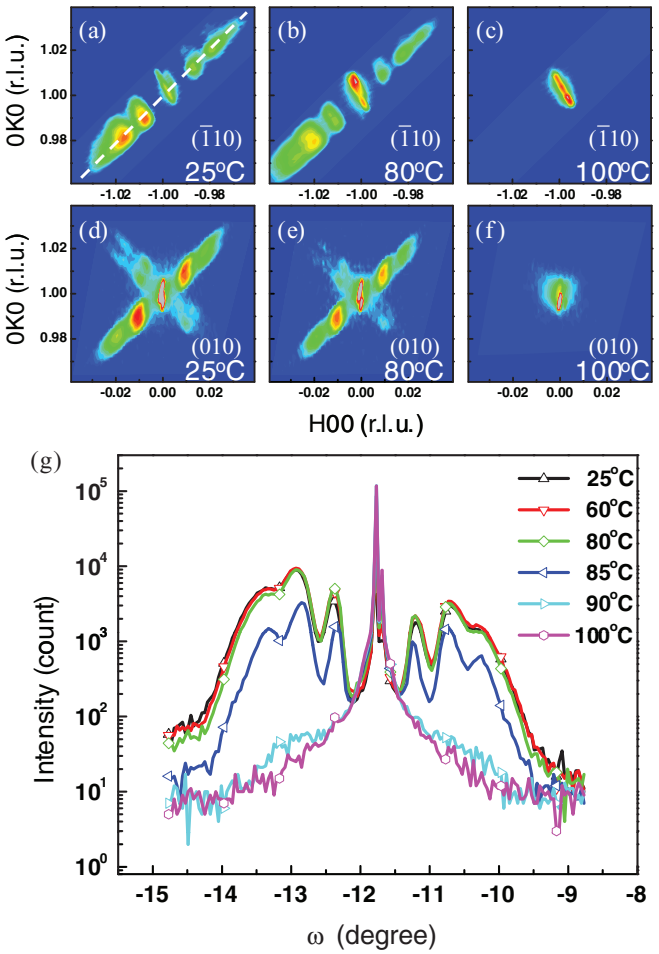

FIG. 5. (Color online) (a)–(c) ($\bar{1}10$) RSMs, (d)–(f) (010) RSMs, and (g) the corresponding line scans of a 12-nm-thick BFO film at different temperatures. The dotted line in (a) indicates the trail of the line scans.

phase. Eventually all these peaks vanish at 90 °C. Some supporting evidence is available in recent reports,[33–36,47,48] which show that the film becomes T-like M_A phase above 90 °C. Such M_C-M_A structural transition near room temperature has been detected in very recent studies by different techniques, such as Raman spectroscopy,[33] neutron diffraction,[34] TEM,[48] and PFM.[36,47] Our experimental result presented here unambiguously shows that both the crystal and domain structures of T-like BFO undergo a phase transition at ∼90 °C. Since the crystal symmetry and domain structure (including domain walls) play an important role on the unique physical properties of BFO, this near-room-temperature structural and domain pattern's change will lead to various controllable functionalities in BFO, such as magnetoelectric properties. The disappearance of satellite spots in the XRD pattern above the M_C-M_A phase transition temperature further confirms that the satellite peaks in the GIXRD patterns originate from periodic polar domains rather than other periodic defects, such as dislocations.

IV. CONCLUSION

In summary, high-resolution synchrotron XRD studies reveal the existence of periodic elastic nanodomains in pure T-like BFO/LAO epitaxial films with thickness down to 6 nm. A unique strain-accommodation mechanism is disclosed, where the adjacent T-like BFO domains adopt small antiphase in-plane rotations to match better with each other as well as with the substrate along the diagonal. The domain size increases with film thickness at a power law constant ∼0.75 and deviates from the classical square root law. Temperature-dependent studies show that the periodic nanodomain modulation vanishes when a structural transition occurs from T-like M_C phase to T-like M_A phase at ∼90 °C. This correlates the evolution of domain structure with intriguing near-room-temperature magnetic and ferroelectric property changes discovered very recently in highly strained BFO films.[33–36] These findings not only enrich the understanding of the nature of T-like BFO, but also underscore the unique power of synchrotron XRD for the determination of polar symmetry, domain structure, and strain-accommodation mechanism in ferroic ultrathin films.

ACKNOWLEDGMENTS

We are grateful to Dr. Ping Yang and Dr. Dillon Fong for useful discussions. This work was supported by the National Basic Research Program of China (973 program) (Grants No. 2010CB934501 and No. 2012CB922004), the Natural Science Foundation of China (Grants No. 11004178, No. 11179008, No. 51021091, and No. 50832005), and the Chinese Universities Scientific Fund. Z.C. acknowledges the support from the Ian Ferguson Postgraduate Fellowship. L.C. acknowledges the support from the Singapore National Research Foundation under the CREATE program: Nanomaterials for Energy and Water Management, 9th Thousand Talent Program of China, and a start-up fund from SUSTC. The work at NCTU is supported by the National Science Council, R.O.C (Grant No. NSC-101–2119-M-009–003-MY2), Ministry of Education (Grant No. MOE-ATU 101W961), and Center for interdisciplinary science of National Chiao Tung University. The authors thank beamline U7B of NSRL and beamlines BL14B1, BL08U of SSRF for providing the beam time.

*zlluo@ustc.edu.cn
†These authors contributed equally to this work.
‡chenlang@sustc.edu.cn
§cgao@ustc.edu.cn

[1] J. F. Scott, Science **315**, 954 (2007).
[2] A. K. Tagantsev, L. E. Cross, and J. Fousek, *Ferroelectric Domains in Ferroelectric Crystals and Thin Films* (Springer, New York, 2010).
[3] A. L. Roitburd, Phys. Status Solidi A **37**, 329 (1976).
[4] A. L. Roytburd and Y. Yu, Ferroelectrics **144**, 137 (1993).

[5]A. L. Roytburd, Phase Transitions **45**, 1 (1993).
[6]W. Pompe, X. Gong, Z. Suo, and J. S. Speck, J. Appl. Phys. **74**, 6012 (1993).
[7]K. Lee and S. Baik, Annu. Rev. Mater. Res. **36**, 81 (2006).
[8]A. Vlooswijk, B. Noheda, G. Catalan, A. Janssens, B. Barcones, G. Rijnders, D. H. A. Blank, S. Venkatesan, B. Kooi, and J. T. M. de Hosson, Appl. Phys. Lett. **91**, 112901 (2007).
[9]V. Nagarajan, A. Roytburd, A. Stanishevsky, S. Prasertchoung, T. Zhao, L. Chen, J. Melngailis, O. Auciello, and R. Ramesh, Nat. Mater. **2**, 43 (2003).
[10]S. Kim, S. Hishita, Y. M. Kang, and S. Baik, J. Appl. Phys. **78**, 5604 (1995).
[11]Y.-H. Chu, M. P. Cruz, C.-H. Yang, L. W. Martin, P.-L. Yang, J.-X. Zhang, K. Lee, P. Yu, L.-Q. Chen, and R. Ramesh, Adv. Mater. **18**, 2307 (2006).
[12]A. Duk, M. Schmidbauer, and J. Schwarzkopf, Appl. Phys. Lett. **102**, 091903 (2013).
[13]J. Lettieri, Y. Jia, M. Urbanik, C. I. Weber, J.-P. Maria, and D. G. Schlom, Appl. Phys. Lett. **73**, 2923 (1998).
[14]G. Catalan, J. Seidel, R. Ramesh, and J. F. Scott, Rev. Mod. Phys. **84**, 119 (2012).
[15]J. Seidel, L. W. Martin, Q. He, Q. Zhan, Y. H. Chu, A. Rother, M. E. Hawkridge, P. Maksymovych, P. Yu, M. Gajek, N. Balke, S. V. Kalinin, S. Gemming, F. Wang, G. Catalan, J. F. Scott, N. A. Spaldin, J. Orenstein, and R. Ramesh, Nat. Mater. **8**, 229 (2009).
[16]M. Daraktchiev, G. Catalan, and J. F. Scott, Phys. Rev. B **81**, 224118 (2010).
[17]Y. Qi, C. Huang, Z. H. Chen, Z. L. Luo, Y. Wang, J. Guo, T. White, J. Wang, C. Gao, T. Sritharan, and L. Chen, Appl. Phys. Lett. **99**, 132905 (2011).
[18]S. K. Streiffer, J. A. Eastman, D. D. Fong, C. Thompson, A. Munkholm, M. V. Ramana Murty, O. Auciello, G. R. Bai, and G. B. Stephenson, Phys. Rev. Lett. **89**, 067601 (2002).
[19]D. D. Fong, G. B. Stephenson, S. K. Streiffer, J. A. Eastman, O. Auciello, P. H. Fuoss, and C. Thompson, Science **304**, 1650 (2004).
[20]G. Catalan, A. Janssens, G. Rispens, S. Csiszar, O. Seeck, G. Rijnders, D. H. A. Blank, and B. Noheda, Phys. Rev. Lett. **96**, 127602 (2006).
[21]G. Rispens, Ph.D. thesis, University of Groningen, 2010.
[22]G. Catalan and J. F. Scott, Adv. Mater. **21**, 2463 (2009).
[23]F. Zavaliche, S. Y. Yang, T. Zhao, Y. H. Chu, M. P. Cruz, C. B. Eom, and R. Ramesh, Phase Transitions **79**, 991 (2006).
[24]C. Ederer and N. A. Spaldin, Phys. Rev. Lett. **95**, 257601 (2005).
[25]H. Béa, B. Dupé, S. Fusil, R. Mattana, E. Jacquet, B. Warot-Fonrose, F. Wilhelm, A. Rogalev, S. Petit, V. Cros, A. Anane, F. Petroff, K. Bouzehouane, G. Geneste, B. Dkhil, S. Lisenkov, I. Ponomareva, L. Bellaiche, M. Bibes, and A. Barthélémy, Phys. Rev. Lett. **102**, 217603 (2009).
[26]R. J. Zeches, M. D. Rossell, J. X. Zhang, A. J. Hatt, Q. He, C. H. Yang, A. Kumar, C. H. Wang, A. Melville, C. Adamo, G. Sheng, Y. H. Chu, J. F. Ihlefeld, R. Erni, C. Ederer, V. Gopalan, L. Q. Chen, D. G. Schlom, N. A. Spaldin, L. W. Martin *et al.*, Science **326**, 977 (2009).
[27]Z. H. Chen, Z. L. Luo, C. Huang, Y. Qi, P. Yang, L. You, C. Hu, T. Wu, J. Wang, C. Gao, T. Sritharan, and L. Chen, Adv. Funct. Mater. **21**, 133 (2011).
[28]Z. Chen, L. You, C. Huang, Y. Qi, J. Wang, T. Sritharan, and L. Chen, Appl. Phys. Lett. **96**, 252903 (2010).
[29]C.-S. Woo, J. H. Lee, K. Chu, B.-K. Jang, Y.-B. Kim, T. Y. Koo, P. Yang, Y. Qi, Z. Chen, L. Chen, H. C. Choi, J. H. Shim, and C.-H. Yang, Phys. Rev. B **86**, 054417 (2012).
[30]H. M. Christen, J. H. Nam, H. S. Kim, A. J. Hatt, and N. A. Spaldin, Phys. Rev. B **83**, 144107 (2011).
[31]Z. H. Chen, Z. L. Luo, Y. Qi, P. Yang, S. Wu, C. Hu, T. Wu, J. Wang, C. Gao, T. Sritharan, and L. Chen, Appl. Phys. Lett. **97**, 242903 (2010).
[32]J. X. Zhang, Q. He, M. Trassin, W. Luo, D. Yi, M. D. Rossell, P. Yu, L. You, C. H. Wang, C. Y. Kuo, J. T. Heron, Z. Hu, R. J. Zeches, H. J. Lin, A. Tanaka, C. T. Chen, L. H. Tjeng, Y.-H. Chu, and R. Ramesh, Phys. Rev. Lett. **107**, 147602 (2011).
[33]I. C. Infante, J. Juraszek, S. Fusil, B. Dupé, P. Gemeiner, O. Diéguez, F. Pailloux, S. Jouen, E. Jacquet, G. Geneste, J. Pacaud, J. Íñiguez, L. Bellaiche, A. Barthélémy, B. Dkhil, and M. Bibes, Phys. Rev. Lett. **107**, 237601 (2011).
[34]G. J. MacDougall, H. M. Christen, W. Siemons, M. D. Biegalski, J. L. Zarestky, S. Liang, E. Dagotto, and S. E. Nagler, Phys. Rev. B **85**, 100406 (2012).
[35]W. Siemons, M. D. Biegalski, J. H. Nam, and H. M. Christen, Appl. Phys. Express **4**, 095801 (2011).
[36]Ko, M. H. Jung, Q. He, J. H. Lee, C. S. Woo, K. Chu, J. Seidel, B. Jeon, Y. S. Oh, K. H. Kim, W. Liang, H. Chen, Y. Chu, Y. H. Jeong, R. Ramesh, J. Park, and C. Yang, Nat. Commun. **2**, 567 (2012).
[37]Z. H. Chen, S. Prosandeev, Z. L. Luo, W. Ren, Y. Qi, C. W. Huang, L. You, C. Gao, I. A. Kornev, T. Wu, J. Wang, P. Yang, T. Sritharan, L. Bellaiche, and L. Chen, Phys. Rev. B **84**, 094116 (2011).
[38]L. You, Z. H. Chen, X. Zou, H. Ding, W. Chen, L. Chen, G. Yuan, and J. L. Wang, ACS Nano **6**, 5388 (2012).
[39]Z. H. Chen, X. Zou, W. Ren, L. You, C. W. Huang, Y. R. Yang, P. Yang, J. L. Wang, T. Sritharan, L. Bellaiche, and L. Chen, Phys. Rev. B **86**, 235125 (2012).
[40]See Supplemental Material at http://link.aps.org/supplemental/10.1103/PhysRevB.88.064103 for methods and supplemental data.
[41]U. Gebhardt, N. V. Kasper, A. Vigliante, P. Wochner, H. Dosch, F. S. Razavi, and H.-U. Habermeier, Phys. Rev. Lett. **98**, 096101 (2007).
[42]N. A. Pertsev and A. G. Zembilgotov, J. Appl. Phys. **78**, 6170 (1995).
[43]M. Hehn, S. Padovani, K. Ounadjela, and J. P. Bucher, Phys. Rev. B **54**, 3428 (1996).
[44]C. W. Huang, Z. H. Chen, and L. Chen, J. Appl. Phys. **113**, 094101 (2013).
[45]C. Kittel, Phys. Rev. **70**, 965 (1946); Rev. Mod. Phys. **21**, 541 (1949).
[46]T. Mitsui and J. Furuichi, Phys. Rev. **90**, 193 (1953).
[47]H. J. Liu, C. W. Liang, Wen-I Liang, H. J. Chen, J. C. Yang, C. Y. Peng, G. F. Wang, F. N. Chu, Y. C. Chen, H. Y. Lee, L. Chang, S. J. Lin, and Y. H. Chu, Phys. Rev. B **85**, 014104 (2012).
[48]Y. J. Qi, Z. H. Chen, L. H. Wang, X. D. Han, J. L. Wang, T. Sritharan, and L. Chen, Appl. Phys. Lett. **100**, 022908 (2012).